Article:

Q1 Formation of polyphenol-based nanoparticles in dried hawthorn with enhanced cellular ~~in vitro~~ absorption over free polyphenols

Q2

ⓘ Corrections to the list or order of authors will require written approval from all authors and is subject to approval from the journal's editor. This may delay the publication of your article.

Xiangyu Meng[a,1], Sihao Luo[b,1], Zhaoshuo Yu[a,c,d,*], zhaoshuo.yu1@ucdconnect.ie, Fangzhou He[e], Hanlin Xu[a], Xuanlu Jin[b], Lijing Ke[e], Jianwu Zhou[f,g], Huaiyu Gu[g,h], Pingfan Rao[f,f,g], Patrick Wall[c,d]

[a]UCD School of Agriculture and Food Science, University College Dublin, Belfield, Dublin 4, Ireland

[b]SIBS-Zhejiang Gongshang University Joint Centre for Food and Nutrition Sciences, Zhejiang Gongshang University, Hangzhou 310012, China

[c]National Nutrition Surveillance Centre, University College Dublin, Dublin, Ireland

[d]Food for Health Ireland, UCD Institute of Food and Health, University College Dublin, Belfield, Dublin 4, Ireland

[e]School of Food Science and Nutrition, University of Leeds, Leeds LS2 9JT, UK

[f]International Union of Food Science and Technology (IUFoST), Guelph, ON, Canada.

[f,g]College of Food and Bioengineering, Fujian Polytechnic Normal University, Fuqing, Fujian, China

[g,h]Institute of Basic Medical Sciences, Chinese Academy of Medical Sciences, Department of Human Anatomy, Histology and Embryology, School of Basic Medicine, Peking Union Medical College, Beijing 100005, China

*Corresponding author at: UCD School of Agriculture and Food Science, University College Dublin, Belfield, Dublin 4, Ireland.

[1]The authors contributed equally to this work.

Abstract

Plant-derived nanoparticles are gaining attention for enhancing the delivery and bioavailability of bioactive compounds, though the mechanisms remain unclear. This study aims to investigate dried hawthorn-derived nanoparticles (DHNPs), focusing on their composition, molecular interactions and impact on polyphenol absorption. The results showed that DHNPs, averaging 275.7 nm, were primarily composed of polysaccharides and high content of polyphenolic compounds (~25%), with covalent and non-covalent interactions forming between them. Saponification increased the polyphenol release, and metabolomics identified 252 polyphenolic compounds, with 195 showing a relative increase post-treatment, including caffeic acid and (−)-catechin. An *in vitro* intestinal absorption test using Caco-2 cell monolayer model demonstrated that DHNPs-bound polyphenols exhibited significantly higher permeability (27.90%) compared to free polyphenols (12.38%), indicating that endocytosis may serve as a potential pathway through which DHNPs enhance polyphenol absorption. This study provides new insights into the role of plant-derived nanoparticles contributing to bioactive compound delivery and bioavailability.

Keywords:

Dried hawthorn, Nanoparticles, Polyphenol absorption

Data availability

~~Data will be made available on request~~ The authors declare that the data supporting the results of this study are available within the article.

~~1.~~1 Introduction

In the post-pandemic era, there has been a surge in global demand for functional foods, as they not only provide nutrition but also promote health, becoming a key means of supporting well-being. Consequently, the "Food First Strategy"—which advocates for nutritional interventions before pharmaceutical treatments—has gained increasing support, revealing the crucial role of food in health management [1]. China's concept of "medicine and food homology" [2] is a quintessential representation of the "Food First Strategy". This time-tested traditional concept emphasizes that food and medicine share similar therapeutic properties. A notable example is hawthorn (*Crataegus spp.*), which is highly valued for its dual role as both food and medicine [3]. This sweet and tangy berry is processed into a variety of tasty foods, and when dried, its medicinal properties emerge [4], demonstrating clinical effects such as regulating blood lipids, improving gastrointestinal function, and providing anti-inflammatory benefits [5,6]. These therapeutic outcomes are generally attributed to the high content of polyphenolic compounds in hawthorn, particularly compounds such as chlorogenic acid, caffeic acid, and quercetin. Despite increasing evidence supporting the health benefits of polyphenols, their low bioavailability in free form makes it difficult to fully account for the overall efficacy of hawthorn. Although thermal drying is essential in traditional processing, it may degrade heat-sensitive polyphenols, presenting a paradox with the preserved or even enhanced efficacy of dried hawthorn. Yet, the underlying molecular mechanisms remain unexplored.

Polyphenols in real foods or herbal medicines rarely exist in isolation. Beyond their inherent ability to self-assemble—for instance, the multiple hydroxyl groups and benzene rings in polyphenols can lead to micro- and nanoscale structures through π–π stacking and hydrogen bonding—polyphenols also interact with complex food or herb matrices, which can influence their bioavailability and effectiveness [7]. However, the specifics of these interactions and their effects on bioavailability and biological activity have yet to be systematically investigated.

Recent studies show that polyphenols can interact with biomacromolecules *via* covalent or non-covalent bonds, which alters their chemical structure, bioavailability, and biological effects [8–10]. In certain purified polyphenol models, non-covalent interactions between dietary fibers and polyphenols—such as procyanidin B2, phlorizin, and epicatechin—were found to significantly influence polyphenol bioaccessibility and bioavailability, thereby affecting intestinal metabolism [11]. Additionally, hawthorn polyphenol-chitosan nanoparticles showed an improved thermal stability and cellular compatibility compared to free-form hawthorn polyphenols [12].

These effects are seen not only in purified systems but also in real food matrices, where polyphenol-macromolecule interactions become even more complex. Such interactions are influenced by food or herbal processing factors, like high temperatures, optimal pH, and enzymatic reactions, which can accelerate polyphenol binding to biomacromolecule [8,13]. For example, during coffee bean roasting and brewing, carbohydrates and proteins form melanoidin (Maillard reaction products) that bind to polyphenols through covalent bonds, such as ester linkages and glycosylation, resulting in most polyphenols in coffee being bound [14,15]. Similarly, in Mediterranean cuisine, when wine—renowned for its health benefits due to resveratrol in its free form—is commonly cooked with clams, protein-polysaccharide nanoparticles are formed. These nanoparticles non-covalently bind to resveratrol, thereby enhancing its stability, enabling controlled release, and improving its bioavailability [16].

Similar cases have also been observed in East Asia. Bioactive compounds in fresh herbs are often encapsulated within cell membranes, making them difficult to absorb directly. To solve the issues, traditional Chinese medicine has developed various processing and decoction protocols over thousands of years, allowing these compounds to undergo physicochemical reactions with water or other components during boiling. These reactions yield abundant micro/nano-structures [17] that improve stability, potency, immunity, and reduce toxicity [18]. For instance, rice vinegar contains nanoparticles with biomacromolecules as skeleton, effectively loading polyphenols produced during fermentation, scavenging free radicals in mucosal immune cells, and maintaining cellular redox balance [19].

Building on these precedents, this study proposes the core hypothesis that naturally occurring polyphenol-based nanoparticles exist in dried hawthorn, primarily composed of polysaccharides, which interact with polyphenolic compounds, thereby influencing their stability, release properties, and bioavailability. To validate the hypothesis, dried hawthorn-derived nanoparticles (DHNPs) were isolated and characterized to determine particle size and composition. The linkages between polysaccharides and polyphenols were analyzed using ester bond hydrolysis and mass spectrometry, elucidating their role as natural nano-delivery systems. Saponification and metabolomics (both targeted and non-targeted) were employed to profile and quantify polyphenolic compounds before and after treatment. X-ray diffraction (XRD) and *in vitro* simulated release assays were employed to assess the crystallinity and release kinetics of polyphenols in DHNPs. Additionally, a Caco-2 cell monolayer model was established to compare the permeability of free polyphenols and DHNP-bound polyphenols, while endocytosis inhibitors were applied to evaluate the absorption mechanism.

2.2 Materials and methods

2.1.2.1 Materials

All reagents used were of analytical or chromatographic grade. Unless otherwise specified, chemicals were purchased from Sinopharm Chemical Reagent Co., Ltd. (Shanghai, China). Specifically, caffeic acid, chlorogenic acid, hyperoside, morin, trans ferulic acid, and (−)-catechin were all of chromatographic grade, along with bovine serum albumin (BSA), water-soluble vitamin E (Trolox), 2,2'-azobis(2-methylpropionamidine) dihydrochloride (AAPH), 1,1-diphenyl-2-picrylhydrazyl (DPPH), sodium fluorescein, L-glutamine, wortmannin, dimethyl sulfoxide (DMSO), and trypsin were purchased from Sigma-Aldrich Co. Ltd. (Shanghai, China). DMEM medium, fetal bovine serum (FBS), penicillin-streptomycin solution, and Hank's balanced salt solution (HBSS) were obtained from Thermo Fisher Scientific (USA). Ultrapure water was prepared using a Milli-Q water purification system. The MTT cell proliferation assay kit was purchased from Nanjing Jiancheng Bioengineering Institute (Nanjing, China).

2.2 Preparation of dried hawthorn

The hawthorn fruits were provided by Fujian Hongguobao Health Industry Co., Ltd. and met the standards of the *Pharmacopoeia of the People's Republic of China* (2020 edition). Fresh hawthorn fruits were washed, sliced into 0.3 cm pieces, and dried in an oven (DHG-9240A, Zhongke Boda Instrument Technology Co., China, Beijing) at 60 °C the moisture content reached 0.12 ± 0.02 g H$_2$O/g dry weight. The slices were then dried at 180–220 °C for 15 min until the surfaces turned dark brown and the interiors became yellow-brown [4,20]. After cooling, the slices were ground into a powder and sieved through a 100-mesh screen.

Dried hawthorn powder (55 g) was mixed with 1 L of deionized water and extracted in a water bath at 100 °C for 30 min with constant stirring. After cooling, the mixture was filtered through gauze and centrifuged at 5000 g, 25 °C for 30 min to remove insoluble residues. The supernatant was collected, freeze-dried to obtain the dried hawthorn extract powder, and stored at −20 °C for future use.

2.3 Isolation of nanoparticles from dried hawthorn

2.0 g of dried hawthorn extract powder was dissolved in deionized water (1:10, *w/v*), mixed, and centrifuged at 5000 g, 4 °C for 15 min. The supernatant was filtered using an ultrafiltration centrifuge tube (15 mL, MWCO: 100 kDa, Millipore, USA) at 5000 g, 25 °C. After each ultrafiltration, the retentate was restored to its original volume and the process was repeated three times. The final retentate was collected as dried hawthorn nanoparticles (DHNPs) and stored at −20 °C for future analysis.

2.4 Characteristics of dried hawthorn nanoparticles of DHNPs

The average size, ζ-potential, and polydispersity index (PDI) of DHNPs were measured using the Zetasizer Nano ZS90 (Malvern Instruments Ltd., Worcestershire, UK). A viscosity of 0.8872 and refractive index (RI) of 1.330 were used in the measurement and analysis. The morphology of DHNPs was observed using transmission electron microscopy (TEM, Hitachi 7650, Tokyo, Japan).

2.5 Composition analysis of DHNPs

2.5.1 Total soluble solid.

The total soluble solid content of DHNPs was determined using a freeze-drying method. The DHNPs were freeze-dried in a freeze dryer (VCP63MV, CHRIST, Germany), and their weight was accurately measured after drying.

2.5.1 Total protein content

The protein content of DHNPs was measured using the Coomassie Brilliant Blue method [21]. Briefly, Coomassie Brilliant Blue was dissolved in 95 % ethanol, mixed with 85 % phosphoric acid, diluted and filtered for use. A 100 μL sample or bovine serum albumin (BSA) was added to the reagent and incubated for 2–5 min. The absorbance at 595 nm was measured using a UV–Vis spectrophotometer (U-5100, Shimadzu, Japan).

2.5.2 Reducing sugar content

The reducing sugar content in DHNPs was measured using the DNS reagent [22]. DNS reagent was prepared by dissolving DNS in a solution of potassium sodium tartrate, phenol, and anhydrous sodium sulfate, followed by the addition 2 mol/L NaOH and heating at 60 °C until fully dissolved. A 1 mL of glucose or sample solution was mixed with 750 μL DNS reagent, boiled for 5 min for color development. After cooling with flowing water, 1.5 mL of distilled water was added, mixed, and the absorbance at 540 nm was measured.

2.5.3 Total carbohydrate content

The total carbohydrate content in DHNPs was measured using the anthrone colorimetric method [23]. Anthrone was dissolved in 80 % H$_2$SO$_4$, and under an ice-water bath, 2 mL of the reagent was added to the glucose standard solution or sample, mixed well, and reacted in a water bath at 100 °C for 10 min. After rapid cooling in an ice-water bath, the absorbance was measured at 620 nm.

[Instruction: 2.5.5] 2.5.4 *Free amino acid analysis*

The free amino acid content in DHNPs was determined using the ninhydrin color reaction method [24]. Using glutamic acid as the standard, 1 mL of the standard or sample solution was added to a colorimetric tube, along with 0.5 mL of PBS solution at pH 8.0 and 0.5 mL of 2 % ninhydrin solution. The mixture was heated in a boiling water bath for 15 min, cooled, and then diluted to a volume of 25 mL with water. After standing for 10 min, the absorbance was measured at 570 nm.

[Instruction: 2.5.6] 2.5.5 *Melanoidin content*

Melanoidin was extracted from DHNPs using the Sevag method [25]. A 20 % (v/v) Sevag reagent was added, stirred for 30 min, and allowed to stand for 2 h. After centrifugation, the supernatant was dialyzed (1 kDa membrane, 48 h) and ultrafiltered (>10 kDa), followed by lyophilization. Quantification was based on a glucose–glycine model system [26]. Briefly, 0.05 mol glucose and glycine were dissolved in 100 mL water, freeze-dried, and heated at 125 °C for 2 h. The resulting powder (5 g) was redissolved, stirred at 4 °C for 12 h, filtered, and freeze-dried to obtain the melanoidin standard. A standard curve (5–100 mg/L) was prepared, and absorbance was measured at 345 nm using a UV–Vis spectrophotometer (U-5100, Shimadzu, Japan).

2.6 Analysis of DHNPs-PC

2.6.1 *Extraction of pectin from DHNPs*

Pectin extraction was modified from Bu et al. [27]. DHNPs were mixed with deionized water (1:10, w/v) and stirred at 90 °C for 4 h. After centrifugation (5000 rpm, 20 min), the supernatant was collected, and twice the volume of 95 % ethanol was added while stirring. The mixture was kept at 4 °C for 12 h to precipitate pectin, which was then centrifuged and washed twice with 95 % ethanol. The pellet was dissolved in a 0.1 mol/L Na_2CO_3/$NaHCO_3$ buffer (pH 7.5) and incubated at 30 °C. The pH was adjusted to 10.0 and maintained for 30 min to remove bound polyphenols. Subsequently, the pH was adjusted to 3.5, and DHNPs-pectin was precipitated with 95 % ethanol, washed twice, freeze-dried and collected as DHNPs-PC.

2.6.2 *Monosaccharide composition of DHNPs-PC*

The monosaccharide composition of DHNPs-PC was determined by strong acid hydrolysis combined with PMP (1-phenyl-3-methyl-5-pyrazolone) derivatization [28]. DHNPs-PC (5 mg/mL) was hydrolyzed with 4 mol/L TFA at 110 °C for 2 h, then dried with methanol under nitrogen at 70 °C. The residue was dissolved in 0.3 mol/L NaOH. For derivatization, 400 µL of sample or standard was mixed with 400 µL PMP-methanol and reacted at 70 °C for 2 h, neutralized with HCl, extracted with chloroform, and filtered (0.45 µm). The aqueous phase was analyzed by HPLC (Agilent 1100, DAD). The relative contents of HG and RG-I domains in pectin were estimated using eq. (1) and (2) based on Bu et al.'s method [27].

$$HG\% = GalA\ (\%) - Rha\ (\%) \tag{1}$$

$$RG - I\% = 2Rha\ (\%) + Gal\ (\%) + Ara\ (\%) \tag{2}$$

2.6.3 *Molecular weight of DHNPs-PC*

The molecular weight of DHNPs-PC was determined using gel permeation chromatography (GPC) equipped with a refractive index detector (Optilab T-rEX) and a multi-angle laser light scattering detector (DAWN HELEOS II) (Wyatt Technology, USA). Separation was performed on Ohpak SB-805 HQ and SB-803 HQ columns (300 × 8 mm, 45 °C) with an isocratic elution of 0.02 % NaN_3 and 0.1 M $NaNO_3$ at 0.6 mL/min for 75 min. DHNPs-PC solution (4 mg/mL) was filtered (0.45 µm) before 100 µL was injected for analysis.

2.6.4 *Determination of methoxyl content*

The methoxyl content of DHNPs-PC was determined by a titration method based on Rodsamran et al. [29]. Briefly, 0.5 g of DHNPs-PC was dissolved in 100 mL of distilled water at 25 °C, stirred for 2 h, then mixed with 1 g of sodium chloride and phenol red indicator. The solution was titrated with 0.1 M NaOH until neutralization, then combined with 25 mL of 0.25 M NaOH and left for 30 min. Subsequently, 25 mL of 0.25 M HCl was added, followed by titration with 0.1 M NaOH. The final NaOH concentration and titration volume were recorded, and the methoxyl content was calculated accordingly to the eq. (3).

$$\text{Methoxyl content } (\%) = \frac{\text{NaOH concentration } (N) \times \text{NaOH volume } (mL) \times 3.1}{\text{Pectin powder } (g)} \qquad (3)$$

2.7 Determination of total flavonoids

The flavonoid content in DHNPs was determined using the aluminum nitrate colorimetric method [30], with rutin as the standard. A 0.5 mL rutin ethanol solution or sample was mixed with 2 mL distilled water and 0.25 mL 5 % (w/v) $NaNO_2$, then left at room temperature for 6 min. Next, 0.25 mL 5 % (w/v) $Al(NO_3)_3$ was added and left for another 5 min. Finally, 1.0 mL 20 % (w/v) NaOH and 5 mL distilled water were added, and after 15 min, absorbance was measured at 510 nm.

2.8 Determination of total polyphenol content

To determine the total polyphenol content and assess bound polyphenols linked by ester bonds in DHNPs, an alkaline saponification treatment was performed [31]. DNHPs (750 μL) were mixed with 750 μL of a 2 mol/L NaOH containing 2 % (w/w) ascorbic acid and 20 mmol/L ethylenediaminetetraacetic acid (EDTA), incubated at 30 °C for 1 h, then adjusted to pH ~1.0 with 5 mol/L HCl. After being stored at 4 °C for 2 h, the mixture was centrifuged to remove the precipitate and pH was restored using 2 mol/L NaOH. The total polyphenol content of DHNPs before or post alkaline saponification treatment was measured using the Folin-Ciocalteu method [21], with gallic acid as the standard. A 1 mL of the standard or sample was mixed with 4 mL Folin-Ciocalteu reagent, left at room temperature for 3–5 min, then reacted with 10 % Na_2CO_3 for 120 min, the absorbance was measured at 765 nm.

2.9 Non-targeted metabolomics analysis of polyphenolic compounds

The method was adapted from Zhong et al. [32]. Briefly, 400 μL of pre- and post-saponified DHNPs (as described in 2.8) were mixed with 1.2 mL of extraction solvent (1:1, methanol/ acetonitrile), vortexed for 30 s, and centrifuged at 12,000 rpm for 10 min at 4 °C. The supernatant was evaporated under vacuum and reconstituted in 300 μL of 70 % methanol, then centrifuged again. Finally, 250 μL of the supernatant was transferred to an injection vial for UPLC-QTOF-MS/MS analysis.

Non-targeted metabolomics analysis was performed using UPLC-QTOF-MS/MS. Separation was conducted on a Waters BEH C18 column (1.7 μm, 2.1 mm × 100 mm) at 40 °C, with a flow rate of 0.4 mL/min and an injection volume of 5 μL. The mobile phase consisted of A: 98 % H_2O, 2 % ACN, 0.1 % FA; and B: 98 % ACN, 2 % H_2O, 0.1 % FA. A 1.5-min equilibration time was inserted between every two injections. A 20-min gradient elution method was applied, with the following gradient settings: 0–0.5 min, 5 % B; 0.5–16 min, linear increase from 5 % B to 100 % B; 16–18.5 min, 100 % B; 18.5–18.6 min, linear decrease from 100 % B to 5 % B; 18.6–20 min, 5 % B. Throughout the analysis, samples were maintained in a 4 °C auto-sampler. Mass spectrometry was performed in MSE mode (50–1000 m/z) with capillary voltages of 3 kV (ESI+) and 2.5 kV (ESI-), ion source at 120 °C, desolvation at 500 °C, and gas flow at 800 L/h. Leucine-enkephalin was used for online mass calibration.

Raw data were acquired using Waters UNIFI software (v1.9) and subsequently processed with Waters Progenesis QI software (v3.0.3.0). Preprocessing included deconvolution, peak picking, alignment, normalization of peak areas, and noise filtering. Mass-to-charge ratio (m/z), retention time (RT), and peak area were extracted for each feature. Background signals were eliminated by comparison with blank samples, and a data matrix was generated. To ensure data quality, features with ≥80 % missing values across all samples were removed, as well as those with a coefficient of variation (CV) ≥30 % in quality control (QC) samples. Compound identification was performed by matching MS/MS fragmentation spectra against multiple public databases, including Metlin (2019), NIST, NPASS, CMAUP, and Foodb-Plant. Matching criteria included precursor ion mass tolerance within 10 ppm, fragment ion tolerance within 20 ppm, and isotope similarity above 80 %. For databases that contain ion mobility information (e.g., Metlin), the collision cross section (CCS) difference was used as an auxiliary matching parameter, with a tolerance threshold of 5 %. Compounds with confident structural annotations were selected for further statistical analysis.

2.10 Targeted metabolomics analysis of polyphenolic compounds

Targeted metabolomics was used to quantify specific polyphenolic compounds in the DHNPs before and after saponification, including caffeic acid, chlorogenic acid, hyperoside, morin, trans-ferulic acid, and (−)-catechin. The system included a hybrid triple quadrupole linear ion trap mass spectrometer (API 4000 Q-TRAP, AB Sciex, USA) equipped with an ESI interface and a HPLC-20 CE system (Shimadzu, Kyoto, Japan). Sample preparation followed the procedure outlined in Section 2.9, with chromatographic and mass spectrometric parameters based on Yao et al. [33]. Briefly, quantification and separation of phenolic compounds were performed on a C18 Zorbax Eclipse Plus column (1.8 μm, 4.6 × 100 mm, Agilent, USA) at 40 °C. The mobile phases A and B consisted of deionized water containing 0.1 % (v/v) acetic acid and acetonitrile, respectively. The injection volume was 5 μL. The gradient

elution program was as follows: 5% B (0–2 min), 5%–15% B (2–4 min), 15%–60% B (4–10 min), 60%–95% B (10–15 min), 95% B (15–16 min), 95%–60% B (16–18 min), and 60%–5% B (18–20 min), with a 2-min re-equilibration at 5% B before the next injection. Ion source parameters were set as follows: ion source temperature at 550 °C, ion spray voltage at 4.5 kV, curtain gas at 35 mL/min, nebulizer gas at 40 mL/min, and heater gas at 45 mL/min. Both standard and sample analyses were performed in negative ion mode. Multiple reaction monitoring (MRM) scanning mode was utilized for the analysis of targeted compounds.

2.11 X-ray diffraction (XRD)

Following the method of a previous study [34], X-ray diffraction analysis of the samples was performed using a Rigaku MiniFlex 600 X-ray diffractometer (Rigaku Ltd., Tokyo, Japan) to assess their crystalline state. The samples were continuously scanned at a rate of 5°/min within the 2θ range of 5–60° at room temperature.

2.12 Antioxidant activity

The antioxidant capacity of the particles was determined using the following methods: Ferric reducing antioxidant power (FRAP), ABTS radical scavenging capacity, DPPH radical scavenging capacity, and Oxygen radical absorbance capacity (ORAC).

2.12.1 FRAP assay

The FRAP assay was performed with slight modifications based on a previous study [35]. A 200 μL working solution was preheated to 37 °C in a 96-well plate, followed by the addition of 20 μL of the diluted sample. After 4 min at room temperature, absorbance at 593 nm was recorded using a microplate reader (FlexStation 3, Molecular Devices, USA). Results were expressed as mmol of Fe^{2+} equivalents/g dry weight (mmol Fe^{2+}/g DW).

2.12.2 ABTS assay

The ABTS assay followed a modified method from a previous study [36]. A 200 μL ABTS working solution was added to a 96-well plate, followed by 10 μL of Trolox standard or sample solution. After 6 min at 30 °C in the dark, the absorbance at 734 nm was recorded. Results were expressed as mmol of Trolox equivalents/g dry weight (mmol TE/g DW).

2.12.3 DPPH assay

The DPPH assay was performed with minor modifications based on Dong et al. [37]. A 100 μL Trolox standard or sample solution was mixed with 100 μL of DPPH ethanol solution in a 96-well plate. After 30 min in the dark at room temperature, absorbance at 517 nm was recorded. Results were expressed as mmol Trolox equivalents/g dry weight (mmol TE/g DW).

2.12.4 ORAC assay

The ORAC assay was performed in a pH 7.4 PBS system, using a modified method [38]. In a black 96-well plate, 25 μL of Trolox standard solution or sample solution was mixed with 150 μL of fluorescein solution and incubated 37 °C for 10 min. After 25 μL of AAPH solution, fluorescence intensity was recorded every 4 min for 40 cycles (excitation: 485 ± 20 nm, emission: 530 ± 20 nm) until baseline. Results were expressed as mmol Trolox equivalents/g dry weight (mmol TE/g DW).

2.13 *In vitro* simulated release

The release characteristics of polyphenols in DHNPs were studied using the membrane dialysis method [16]. Caffeic acid was used as a standard control, with its concentration corresponding to the total polyphenol concentration in DHNPs (1.89 ± 0.11 mg/mL). An 8 mL solution of the standard control or sample was placed into a dialysis bag with a molecular weight cutoff of 8–12 kDa and immersed in 200 mL of 0.02 mol/L PBS buffer. The setup was stirred magnetically at 37 °C. At predetermined time points (0, 15, 30, 45, 60, 75, 90, 105, and 120 min, as well as 4, 8, 12, and 24 h), 3 mL of the dialysis liquid was taken for polyphenol content measurement according to section 2.8 (Method for determination of polyphenol content), to further obtain the release rate.

To better understand the release mechanism of polyphenols, the *in vitro* release behavior was analyzed using four mathematical models for kinetic analysis, including the Zero-order model (4), First-order model (5), Higuchi model (6), and Korsmeyer-Peppas model (7) [39].

$$\text{Zero} - \text{order kinetics} : F = K_0 t \qquad (4)$$

$$\text{First} - \text{order kinetics} : F = 100^* \left(1 - \exp . \left(-K_1 t\right)\right) \qquad (5)$$

$$\text{Higuchi : } F = K_H t^{1/2} \tag{6}$$

$$\text{Korsmeyer} - \text{Peppas : } F = K_{KP} t^n \tag{7}$$

In the equations, F represents the cumulative release rate of polyphenols at time t, while K_0、K_1、K_H and K_{KP} were the kinetic constants for eqs. (4), (5), (6), and (7), respectively. The release exponent n indicates the release mechanism, and the fitness of the release kinetics model was determined by R^2.

2.14. 2.14 Cytotoxicity of DHNPs in Caco-2 cell model

2.14.1 *Cell culture*:

The human colorectal cancer epithelial cell line Caco-2 was obtained from the Stem Cell Bank, Chinese Academy of Sciences (Shanghai, China). Following the method described by Jin et al. [40], Caco-2 cells were cultured in DMEM supplemented with 10 % fetal bovine serum (FBS), 2 mmol/L L-glutamine, 100 U/mL penicillin, and 100 µg/mL streptomycin. The cells were maintained in a humidified incubator at 37 °C with 5 % CO_2, and the culture medium was replaced every 48–72 hours h. Trypsin treatment was performed before the cells reached confluence.

[Instruction: 2.14.2][Instruction: 2.14.2] 2.14.1. 2.14.1 *MTT assay*

The cytotoxicity test was conducted based on previous studies [41,42]. Caco-2 cells were seeded in a 96-well plate at a density of 6×10^4 cells per well and allowed to adhere for 24 hours h. The culture medium was then replaced with fresh medium containing various concentrations of DHNPs (50, 100, 500, 1000, 2000 µg/mL) to evaluate the toxicity of DHNPs on the cells. All samples were diluted in growth medium to achieve the specified concentrations, with the culture medium serving as a blank control. The cells were incubated at 37 °C for 24 hours h. After incubation, the medium was discarded, and MTT (20 µL, 5 mg/mL) was added for a 4-hour h incubation. Subsequently, 150 µL DMSO was added to release the dye from the cells. The absorbance was measured at 570 nm using a FlexStation 3 microplate reader (Molecular Devices, USA). The concentrations of DHNPs that exhibited no cytotoxic effects were selected for subsequent cell permeability assessments, along with the corresponding concentrations of the coffee acid standard. Cell viability was calculated using the following formula:

$$\text{Cell viability (\%)} = \frac{A_{570nm}\text{sample}}{A_{570nm}\text{control}} \times 100\% \tag{8}$$

2.15. 2.15 Permeability tests based on Caco-2 Ccell Mmonolayers

The permeation rate of caffeic acid from DHNPs were measured using the Caco-2 monolayer cell model [43,44]. Caco-2 cells were seeded at a density of $2-4 \times 10^4$ cell/cm^2 onto 12-well transwell plate inserts (BD Biosciences, USA) with a diameter of 10.5 mm and a pore size of 0.4 µm. The cells were incubated in a humidified environment at 37 °C with 5 % CO_2, with fresh culture medium replaced every day and 24 hours h prior to the experiment. After 20 days, a monolayer was formed, during which the transepithelial electrical resistance (TEER) was measured using the Millicell ERS-2 Voltohmmeter (Millipore, Darmstadt, Germany) to assess monolayer integrity. The procedure involved discarding culture medium solution on both apical and basolateral sides and replacing it with preheated HBSS buffer at 37 °C on both sides. The cells were incubated at 37 °C in a 5 % CO_2 environment for 30 minutes min before TEER measurement. The TEER of culture solutions were detected every 3 days. A TEER value exceeding 250 Ω·cm^2 indicated that the membrane was suitable for experimentation. TEER values were calculated using Eq. (9).

$$\text{TEER} = (R - R_0) \times A \tag{9}$$

Where R was the resistance value of the Transwell of inoculated cells, R_0 was the resistance value of the Transwell of uninoculated cells, and A was the effective surface area.

On the 21st day, the experiment commenced by adding 0.5 mL of the sample to the apical side of the transwell, while 1.5 mL of HBSS buffer was added to the basal side. The system was incubated at 37 °C with 5 % CO_2 for 2 hours h, after which the HBSS buffer from the basal side was collected [45]. The caffeic acid content in the collected buffer was analyzed using HPLC (Agilent 1260, Agilent Technologies, CA, USA). The analysis was achieved with an Agilent

ZORBAX Eclipse Plus C18 column (250 mm × 4.6 mm, Agilent, USA) at a flow rate of 0.5 mL/min. The mobile phase A consisted of water (99.5 %) and acetic acid (0.5 %), while mobile phase B comprised methanol (99.0 %), water (0.5 %), and acetic acid (0.5 %). The elution program was set as follows: B (5 %, 0–5 min), B (25 %, 5–10 min), and B (40 %, 10–30 min). The permeation rate of caffeic acid was calculated based on the HPLC results using the following formula:

$$\text{Permeability } (\%) = \frac{A'}{A} \times 100\% \tag{10}$$

Where A' was the concentration of caffeic acid detected in the HBSS buffer on the basolateral side, and A was the concentration of total caffeic acid detected in the DHNPs particles, or the original free caffeic.

2.16. 2.16 Transport mechanism of DHNPs

Endocytosis, the process by which cells transport extracellular substances into the cell through deformation of the plasma membrane, is crucial for understanding the biological processes of nutrient uptake [46]. To investigate whether the cellular uptake of DHNPs involves endocytosis, Caco-2 cell uptake assays were conducted based on a previous study [41]. A culture medium containing 2 μmol/L of the endocytosis inhibitor Wortmannin was added to the apical side of the cultured cell monolayer and incubated for 1 hour h. Afterward, the medium containing the inhibitor was removed, and 0.5 mL of the sample to be tested was added to the apical side, while 1.5 mL of HBSS buffer was added to the basolateral side. The system was incubated at 37 °C with 5 % CO_2 for 2 hours h. Following incubation, the HBSS buffer from the basolateral side was collected for caffeic acid determination. The permeation rate of caffeic acid was calculated using formula (9 10).

### 2.17. 2.17 Statistical analysis

All experiments in this study were performed in triplicate, and all measurement data were presented as the mean ± standard deviation (SD). Data visualization was conducted using GraphPad Prism 6.0 (GraphPad Software, Inc., USA). Statistical analysis was performed with SPSS software (version 21.0), and the significance of differences among data was evaluated using one-way analysis of variance (ANOVA) with a significance level set at $p < 0.05$.

3. 3 Results and discussion

3.1. 3.1 Characterization of DHNPs

As shown in Fig. 1a and Table 1, the particle size of dried hawthorn nanoparticles (DHNPs) predominantly ranged from 100 to 1000 nm, with a Z-average diameter of 275.70 ± 1.47 nm. Particles smaller than 100 nm and larger than 1000 nm accounted for 13.88 % and 24.98 %, respectively. The zeta potential of DHNPs was measured at 5.44 ± 0.16 mV, indicating that the nanoparticles isolated through ultrafiltration had a slightly negative surface charge.

> ℹ Images may appear blurred during proofing as they have been optimized for fast web viewing. A high quality version will be used in the final publication. Click on the image to view the original version.

alt-text: Fig. 1

Fig. 1. Fig. 1
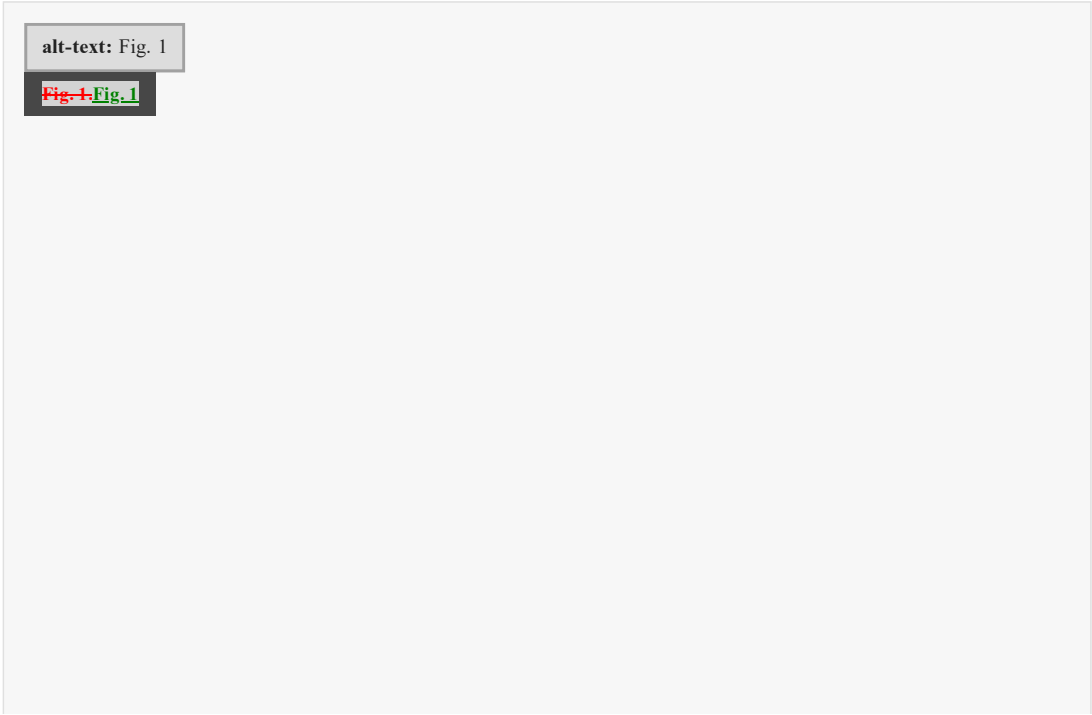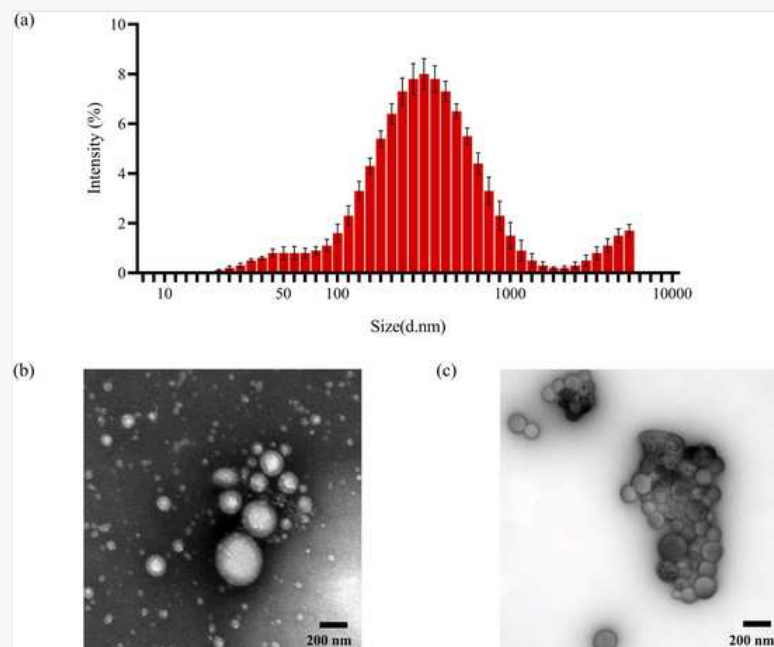
(a) Particle size distribution of DHNPs; (b) and (c) TEM image of DHNPs.

alt-text: Table 1

~~Table 1.~~ Table 1

Particle size, Zeta potential, and Polydispersity Index (PDI) of DHNPs.

	Particle size (nm)	Zeta potential (mV)	PDI
DHNPs	275.70 ± 1.47	−5.44 ± 0.16	0.427 ± 0.01

The morphology of DHNPs was observed by TEM. Fig. 1b showed that DHNPs were primarily spherical, with a particle distribution similar with the Z-average diameter. Fig. 1c confirmed the presence of micro-aggregates within the DHNPs composition, where individual nanoparticles were distinctly visible and remained independent without fusion. Notably, these micro-aggregates could be readily dispersed by ultrasonic treatment, indicating that the system is relatively uniform and stable. This observation suggests that these micro-aggregates within hawthorn were formed through the orderly stacking of multiple nanoparticles, potentially exhibiting a certain degree of crystalline-like order and physical stability.

~~3.2.~~ 3.2 DHNPs composition

To analyze the chemical composition of DHNPs, the concentrations of protein, total sugars, reducing sugars, polyphenols, flavonoids, total acids, and free amino acids were measured, as summarized in Table 2. The total dry matter concentration of DHNPs was 29.65 ± 0.26 mg/mL, with carbohydrates accounting for 60.89 % of the total

composition, including 13.96 % reducing sugars and around 50 % polysaccharides, indicating that polysaccharides were the dominant component in DHNPs. Polyphenolic compounds (total polyphenols and flavonoids) were the second most abundant, accounting for 24.87 %, suggesting that DHNPs were primarily composed of a complex of polysaccharides and polyphenols, consistent with the results of Ding et al. [47]. Additionally, proteins, total acids, and free amino acids together accounted for 5 % of the total composition. This relatively low percentage was likely due to the involvement of proteins in Maillard reaction complexes.

> The table layout displayed in this section is not how it will appear in the final version. The representation below is solely purposed for providing corrections to the table. To view the actual presentation of the table, please click on the ⟳ **Preview** located at the top of the page.

alt-text: Table 2

Table 2. Table 2

Composition of DHNP.

Components	Concentration (mg/mL)	Composition (%)
Total protein	0.48 ± 0.01	1.63 ± 0.01
Total carbohydrate	18.05 ± 0.99	60.89 ± 3.34
Reducing sugar	4.14 ± 0.23	13.96 ± 0.80
Free amino acids	0.44 ± 0.01	1.47 ± 0.01
Polyphenols	3.93 ± 0.17	12.25 ± 0.57
Flavonoids	3.74 ± 0.20	12.62 ± 0.67
Melanoidins	7.37 ± 0.83	24.86 ± 2.80
Dry weight	29.65 ± 0.26	—

Notably, melanoidins, formed as carbohydrate-protein reaction products, accounted for approximately 25 % of the total composition. Interestingly, the combined content of melanoidins, carbohydrates, polyphenols, and proteins exceeded 100 %. This suggests that these components were not present as independent entities but rather existed as complexes. Furthermore, polyphenolic compounds in DHNPs comprised nearly 25 % of the composition, and this high polyphenol content enhanced their potential as natural candidates for nanoparticle-based delivery systems.

3.3. 3.3 Analysis of DHNPs-PC

As shown in Table 3, the primary monosaccharide composition of DHNPs-PC included galacturonic acid (GalA), galactose (Gal), and neutral sugars such as arabinose (Ara), rhamnose (Rha), mannose (Man), and xylose (Xyl). The calculated HG and RG-I contents were 74.2 % and 10.6 %, respectively, indicating that DHNPs-PC is predominantly composed of HG-type pectin, which aligns with previous study reported by Roman et al. [48] and Sun et al. [49].

> The table layout displayed in this section is not how it will appear in the final version. The representation below is solely purposed for providing corrections to the table. To view the actual presentation of the table, please click on the ⟳ **Preview** located at the top of the page.

alt-text: Table 3

Table 3. Table 3

Methoxyl content, molecular wight and monosaccharide composition of DHNPs-PC.

Physicochemical indexes	DHNPs-PC
GalA (%)	75.73 ± 2.1
Methoxyl content (%)	4.78 ± 0.09
Monosaccharide composition	

Rha (%)	1.55 ± 0.04
Ara (%)	6.61 ± 0.11
Xyl (%)	0.74 ± 0.03
Man (%)	0.74 ± 0.03
Gal (%)	0.85 ± 0.06
HG (%)	74.18
RG-I (%)	10.56
(Ara + Gal)/Rha	4.81
Molecular weight	
Mw (kDa)	303.42
Mn (kDa)	93.5
Mw/Mn	3.25

Pectin, a complex polysaccharide, primarily consists of homogalacturonan (HG), rhamnogalacturonan I (RG-I), and rhamnogalacturonan II (RG-II). HG is composed entirely of galacturonic acid residues, whereas RG-I features a repeating disaccharide backbone of alternating non-methyl-esterified galacturonic acid and rhamnose residues, with galactose and arabinose side branches attached to rhamnose [50]. To further assess the branching complexity of RG-I, the (Ara + Gal)/Rha ratio is commonly used as an indicator of side chain length and structural complexity [51]. In DHNPs-PC, this ratio was 4.81, suggesting that the RG-I side chains DHNPs-PC of were relatively short with minimal branching, making the overall structure closer to HG-type pectin.

DHNPs-PC had a methoxyl content of 4.8 %, which was lower than the threshold for high-methoxyl pectin (typically 8–11 %), classifying it as low-methoxyl pectin (LMP). Furthermore, the molecular weight (Mw) of DHNPs-PC was determined to be 303.42 kDa, with a polydispersity index (Mw/Mn) of 3.25, indicating a broad molecular weight distribution and relatively high molecular weight. These characteristics are consistent with previously reported low-methoxyl HG-type hawthorn pectin extracted *via* hot water extraction, which exhibited a molecular weight of 348.43 kDa, a polydispersity index of 2.25, and an HG content of 81 %.

Therefore, based on its high HG content (74.2 %), low RG-I content (10.6 %), low methoxyl content (4.8 %), and relatively high molecular weight (303.42 kDa), DHNPs-PC were supposed be classified as low-methoxyl HG-type pectin.
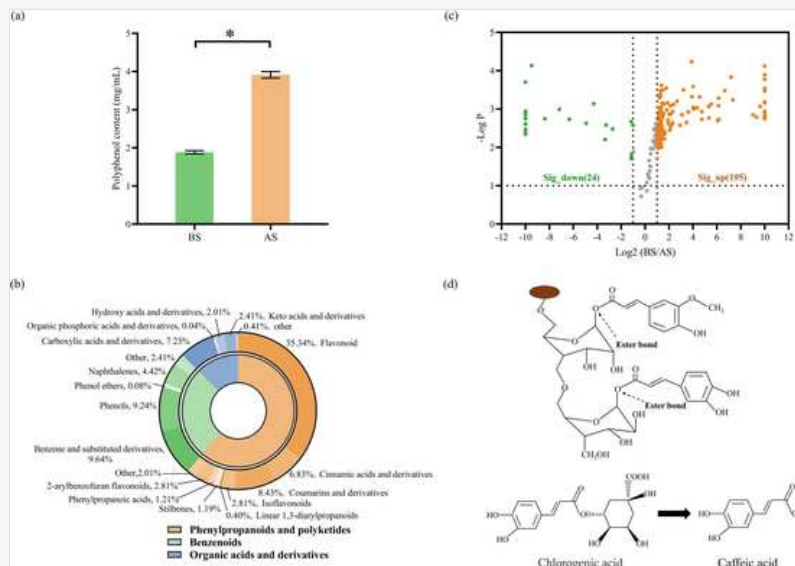
3.4. 3.4 Analysis of polyphenol content in DHNPs before and after saponification

Given that some polyphenols may be bound by chemical bonds within DHNPs, the total polyphenol content in DHNPs were then determined. Saponification was employed to hydrolyze ester alike bonds, thereby to release polyphenols that might be covalently bound to components such as polysaccharides and proteins. Polyphenol content analysis (Fig. 2a) showed that the polyphenol concentration in DHNPs was 1.89 ± 0.11 mg/mL before saponification, increasing to 3.93 ± 0.17 mg/mL after saponification. This increase indicated that a substantial proportion of polyphenols in DHNPs existed in a covalently bound form, often referred to as bound polyphenols. These compounds were typically linked to components such as dietary fibers, cell walls, and polysaccharides through covalent bonds, including ester, glycosidic, or ether linkages [32]. In this study, the significant release of polyphenols following saponification suggested that ester bonds are the predominant type of covalent interaction stabilizing polyphenols within the DHNP matrix. Fig. 2d illustrated a schematic representation of this mechanism, showing the cleavage of ester bonds between polyphenols and polysaccharides in DHNPs during saponification, leading to polyphenol release and nanoparticle disassembly. In contrast, the pre-saponification polyphenol content likely reflected polyphenols adsorbed onto DHNPs through weak interactions, such as hydrogen bonds, intermolecular forces, or hydrophobic interactions.

ℹ Images may appear blurred during proofing as they have been optimized for fast web viewing. A high quality version will be used in the final publication. Click on the image to view the original version.

alt-text: Fig. 2

Fig. 2 Fig. 2

Chemical analysis and non-targeted metabolomics analysis of polyphenolic compounds. (a) Polyphenol content of DHNPs before and after saponification. BS: before saponification; AS: after saponification. '*'Indicates significant difference, $p < 0.05$; (b) Composition of polyphenolic compounds in DHNPs; (c) Volcano plots comparing the composition of polyphenol before and after saponification; (d) Schematic representation of the cleavage of ester bonds between polyphenols and polysaccharides in DHNPs *via* saponification.

3.5. 3.5 Non-targeted metabolomic analysis of DHNPs

The combination of saponification treatment and UPLC-QTOF-MS/MS analysis was employed to identify the phytochemical compounds in DHNPs. As shown in Fig. 2b, a total of 252 bioactive plant compounds were identified in DHNPs, with phenolic compounds (including flavonoids) accounting for over 35 % of the total. Additionally, certain cinnamic acids and their derivatives, coumarins and their derivatives, benzene and substituted derivatives, as well as phenol ethers, were also classified as phenolic compounds. Fig. 3 provided the mass-to-charge ratio (m/z) information for typical polyphenols and flavonoids identified in representative DHNPs samples.

> ℹ Images may appear blurred during proofing as they have been optimized for fast web viewing. A high quality version will be used in the final publication. Click on the image to view the original version.

alt-text: Fig. 3

Fig. 3. Fig. 3
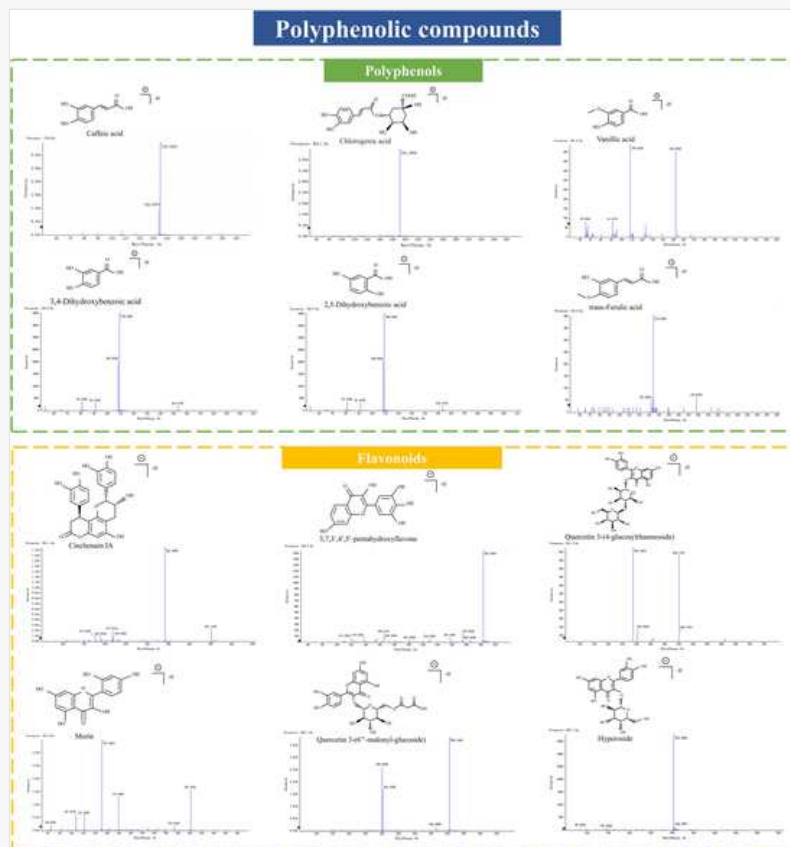
Secondary mass spectra of the main typical compounds in DHNPs.

To clearly illustrate changes in the composition of polyphenolic compounds before and after saponification, a volcano plot (Fig. 2c) was used, where each point represents a compound, and the relative increase or decrease in content was expressed as Log2 (after saponification/before saponification). Table S1 showed the molecular formulas, classifications, mass-to-charge ratios, and relative content variations of all compounds in DHNPs. Based on the data, most phenolic compounds showed an increase in relative content after saponification, including caffeic acid, hyperoside, (-=)-catechin, morin, 2,5-dihydroxybenzoic acid, cinchonain 1a, trans-ferulic acid, and cleomiscosin A. This increase likely explained the overall rise in total polyphenol content (Fig. 2a). The saponification reaction broke the ester bonds and other covalent bonds between the DHNPs matrix and polyphenols (Fig. 2d), leading to an increase in many phenolic compounds, further confirming the presence of covalently bound polyphenols in DHNPs.

Additionally, the relative content of certain phenolic compounds, such as chlorogenic acid, decreased after saponification (Table S1). This reduction was attributed to alkaline saponification breaking the ester bonds within the chlorogenic acid molecule, leading to simpler polyphenolic substances like caffeic acid (Fig. 2d). Carina Coelho et al. suggested that saponification could dissociate both the simple adsorbed and covalently condensed chlorogenic acid in coffee melanoidin, simultaneously degrading it and releasing it as caffeic acid [31], which aligned the results here.

However, this did not suggest the absence of covalently bound chlorogenic acid in DHNPs. Nunes et al. demonstrated that chlorogenic acid and its derivatives in the Maillard reaction products of coffee, particularly in melanoidin fractions, where they existed in a covalently bound form. [52]. On the other hand, carbohydrates, especially arabinose residues, appeared to be potential binding sites for chlorogenic acid derivatives [53]. Moreira et al. confirmed that arabinose residues in arabinogalactan side chains were likely binding sites for chlorogenic acid, identifying sugar-chlorogenic acid covalent compounds formed during thermal processing using electrospray ionization mass spectrometry (ESI-MS) [15]. Given the high content of arabinose in DHNPs, it was highly probable that chlorogenic acid existed in a covalent form within DHNPs, which required further confirmation.

3.6.3.6 Targeted metabolomic analysis of components in DHNPs

To quantify specific polyphenols in DHNPs and further explore the interaction between hawthorn polyphenols and DHNPs, a targeted metabolomic approach was employed based on a triple quadrupole linear ion trap mass

spectrometer. The contents of caffeic acid, chlorogenic acid, hyperoside, morin, trans-ferulic acid, and (-–)-catechin within DHNPs were measured before and after saponification, and the results were shown in Table 4. Saponification led to a significant reduction in chlorogenic acid, with its levels decreasing to 0.35 μg/mg from 4.87 μg/mg. In contrast, the concentrations of caffeic acid, hyperoside, morin, trans-ferulic acid, and (-–)-catechin increased significantly. For example, the concentration of caffeic acid increased from 5.24 to 17.18 μg/mg. As a result, the total content of these compounds rose from 13.30 ± 0.79 μg/mg before saponification to 27.75 ± 2.71 μg/mg after saponification, which aligned with the polyphenol quantification results and non-targeted metabolomics results. Notably, the increase in caffeic acid after saponification was significantly higher than the decrease in chlorogenic acid, with a difference of 7.42 μg/mg. It suggested that the rise in caffeic acid was due not only to the hydrolysis of chlorogenic acid molecules within DHNPs but also to the release of covalently bound chlorogenic acid or caffeic acid within DHNPs.

ℹ️ The table layout displayed in this section is not how it will appear in the final version. The representation below is solely purposed for providing corrections to the table. To view the actual presentation of the table, please click on the ⟳ **Preview** located at the top of the page.

---

alt-text: Table 4

Table 4.Table 4

Quantitative Results of Partial Polyphenols in DHNPs Before and After Saponification.

DHNPs	Phenolic content (μg/mg)						
	Caffeic acid	Chlorogenic acid	Hyperoside	Morin	trans-Ferulic acid	(-–)-Catechin	Total
Before	5.24 ± 0.27^{b}	4.87 ± 0.30 [a]	1.52 ± 0.12 [b]	0.16 ± 0.01 [b]	1.34 ± 0.07 [b]	0.17 ± 0.02 [b]	13.30 ± 0.79 [b]
After	17.18 ± 1.36^{a}	0.35 ± 0.02 [b]	6.34 ± 0.28 [a]	0.29 ± 0.01 [a]	2.11 ± 0.18 [a]	1.48 ± 0.11 [a]	27.75 ± 2.71 [a]

Note: Different superscript characters reveal the significant differences ($p < 0.05$).

Before saponification, the polyphenols in DHNPs were detected due to pre-extraction using organic reagents, such as methanol, which disrupted weak interactions (*e.g.*, hydrogen bonds and van der Waals forces) between polyphenols and the DHNPs matrix. After saponification, which specifically hydrolyzes ester bonds, a higher polyphenol content was determined. This indicates that polyphenols were not only associated with the DHNPs matrix through weak interactions but were also significantly covalently bound to the polysaccharide matrix *via* ester or glycosidic bonds. Furthermore, these results suggest that the thermal drying of hawthorn—from fresh fruit to dried herb—probably modified the molecular structures of polyphenolic compounds, transforming them from a free form into a bound state.

3.7.3.7 X-ray diffraction (XRD) analysis

To verify the state of bioactive polyphenols in DHNPs, the crystallinity of pure caffeic acid, DHNPs, and a simple mixture of caffeic acid and DHNPs were assessed using X-ray diffraction (XRD). As shown in Fig. 4, the XRD pattern of pure caffeic acid displayed several characteristic narrow peaks within the 2θ range of 5-–30°, primarily at 2θ = 15.7, 17.3, and 26.8. The peak shapes of low crystallinity substances were typically broader and shorter, while those of high crystallinity substances were narrower and taller [54]. Pure caffeic acid exhibited a high degree of crystallinity. When DHNPs were simply mixed with caffeic acid, the XRD pattern still showed the characteristic peaks of caffeic acid, although the intensity of these peaks was diminished. In comparison, no characteristic peaks were observed for DHNPs alone. These results suggested that polyphenol-loaded within DHNPs existed in an amorphous, non-crystalline state.

ℹ️ Images may appear blurred during proofing as they have been optimized for fast web viewing. A high quality version will be used in the final publication. Click on the image to view the original version.

---

alt-text: Fig. 4

Fig. 4.Fig. 4
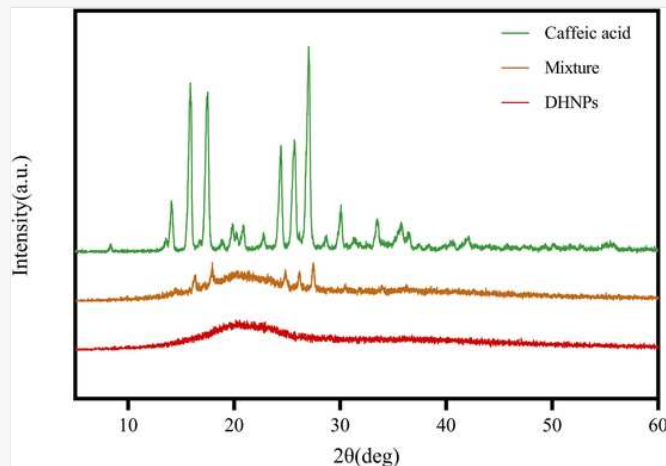
XRD spectra of caffeic acid, DHNPs, and physical mixture of DHNPs/caffeic acid.

When the pure loaded compound interacted with the carrier, it suppressed the crystallization tendency of the compound within the nanostructure, significantly reducing its crystallinity and forming an amorphous composite due to intermolecular interactions [55,56]. Therefore, the structure of DHNPs played a crucial role in encapsulating polyphenols like caffeic acid and altering their crystalline state.

3.8. 3.8 Antioxidant capacity analysis

As shown in Table 5, FRAP of DHNPs was measured at 0.439 ± 0.016 mmol Fe^{2+}/g, while the ABTS, DPPH, and ORAC radical scavenging activities were 0.461 ± 0.018 mmol TE/g, 0.403 ± 0.015 mmol Vc/g, and 1.389 ± 0.106 mmol TE/g, respectively. Phenolic compounds, the main bioactive compounds in hawthorn, play a key role in protecting cells from oxidative damage and promoting health [4]. In a study by García-Alonso et al. [57], the ABTS method was used to assess the antioxidant activities of 28 fruits, with persimmons, blackberries, blueberries, and strawberries showing the strongest antioxidant capacities at 0.406, 0.192, 0.187, and 0.163 mmol TE/g, respectively. All these values were lower than the ABTS scavenging activity of DHNPs (0.461 ± 0.018 mmol TE/g). This evidence indicated that DHNPs, as a natural source of antioxidants, possess strong antioxidant activity.

> ℹ The table layout displayed in this section is not how it will appear in the final version. The representation below is solely purposed for providing corrections to the table. To view the actual presentation of the table, please click on the
> ↻ **Preview** located at the top of the page.

alt-text: Table 5

Table 5. Table 5

Antioxidant Test Results of DHNPs.

Methods	Antioxidant capacity
FRAP (mmol Fe^{2+}/g)	0.439 ± 0.016
ABTS (mmol TE /g)	0.461 ± 0.018
DPPH (mmol Vc /g)	0.403 ± 0.015
ORAC (mmol TE /g)	1.389 ± 0.106

Generally, compared to fresh fruit, thermal processing tends to reduce antioxidant capacity by degrading phenolic compounds [58]. However, Lou et al. measured the antioxidant activity of fresh hawthorn fruits using the FRAP, ABTS, and DPPH methods, with values of 0.32, 0.33, and 0.29 mmol TE/g, respectively which was lower than DHNPs [59]. This suggests that the formation of DHNPs during thermal processing may help stabilize and protect polyphenolic compounds through interactions with polysaccharides, reducing their degradation and enhancing their antioxidant capacity.

3.9. 3.9 *iIn vitro* simulated release

To evaluate the impact of the DHNPs structure on the release of polyphenols, a membrane dialysis method was used with free caffeic acid as a control. As shown in Fig. 5a, free caffeic acid exhibited a burst release within the first 0–2

h, with a release rate exceeding 85 %. Subsequently, the release rate slowed, reaching a cumulative release rate of 92.6 % at 24 h. This phenomenon was likely related to the small molecular size of free caffeic acid and its unobstructed diffusion process [60]. In contrast, caffeic acid loaded in DHNPs displayed a fast release within 0–4 h but at a significantly lower rate compared to free caffeic acid, reaching only 50 % cumulative release at 4 h and a final release rate of 71.2 % at 24 h. These results indicate that DHNPs effectively prolonged the release of caffeic acid, resulting in a sustained-release effect.

alt-text: Fig. 5

Fig. 5. Fig. 5
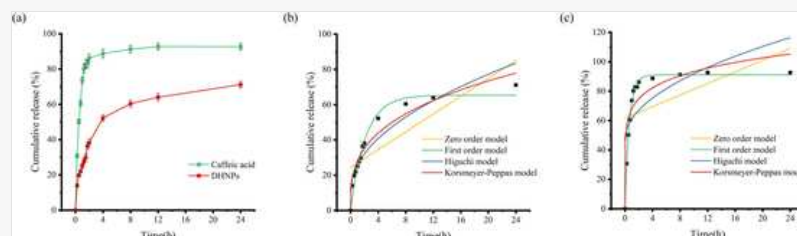
in vitro kinetics and fitting models of polyphenol released from DHNPs. (a) Release curves of DHNPs and pure caffeic acid; (b) Dynamic fitting curve for DHNPs; (c) Dynamic fitting curve for the caffeic acid standard.

To further elucidate the release mechanism, four kinetic models, including Zero-order, First-order, Higuchi, and Korsmeyer-Peppas, were used to fit the release data of caffeic acid (Fig. 5b-c, Table 6). The results showed that the release behavior of both free caffeic acid and DHNP-loaded caffeic acid was well-fitted by the First-order model, with the highest R-squared value (R^2 = 0.997 for free caffeic acid and 0.968 for DHNPs-encapsulated caffeic). This suggested that the release kinetics followed the characteristics of the First-order model, where the release rate was proportional to the remaining amount of unreleased substance [61]. In the First-order model, slope K1 represented the relative release capacity. The K1value of free caffeic acid was 1.578, significantly higher than that of DHNP-encapsulated caffeic acid (0.462). This difference was primarily attributed to the physical encapsulation and chemical interactions between DHNPs and caffeic acid, leading to the sustained-release effect. The nanoparticle structure of the polysaccharide matrix may form a diffusion barrier, slowing the release rate of caffeic acid from the carrier [62]. Analysis of the release curves suggests that this reduction is mainly observed in the initial burst-release phase, where surface-adsorbed caffeic acid is rapidly released, and the diffusion of internally bound caffeic acid gradually dominates the release process, achieving the sustained-release effect.

alt-text: Table 6

Table 6. Table 6

Correlation Coefficients of Three Kinetic Models for the Release of Caffeic Acid and DHNPs.

Samples		Release kinetics model			
		Zero-order	First-order	Higuchi	Korsmeyer-Peppas
Caffeic acid	Equation	Q = 1.977*t + 61.533	Q = 91.037*(1- exp.(- 1.578 t))	Q = 14.200*t$^{1/2}$+ 46.889	Q = 67.932*t$^{0.138}$
	R^2	0.233	0.997	0.468	0.828
DHNPs	Equation	Q = 2.528*t + 24.352	Q = 65.3083*(1- exp.(- 0.462 t))	Q = 14.760*t$^{1/2}$+ 11.203	Q = 28.103*t$^{0.321}$
	R^2	0.672	0.968	0.894	0.954

Additionally, the results showed that the release behavior of caffeic acid from DHNPs was also well correlated with the Korsmeyer-Peppas kinetic model ($R^2 = 0.954$). The release exponent n was 0.321 (< 0.5), indicating that the release of caffeic acid was primarily controlled by Fickian diffusion, where the rate of substance transfer is proportional to the concentration gradient, and was also influenced by factors such as the carrier structure, particle size, diffusion path, and interactions between the carrier and the encapsulated compound [63,64]. These results suggested that the polysaccharide matrix of DHNPs significantly delayed the release of caffeic acid by providing a diffusion barrier and promoting molecular interactions, suggesting its critical role in the sustained release of polyphenolic compounds.

3.10. 3.10 Effects of DHNPs on the cytotoxicity of Caco-2 cells

The cytotoxicity assay results were shown in Fig. 6a. DHNPs at concentrations ranging from 50 to 2000 μg/mL showed no toxic effects on cells. At 50 μg/mL, there was no significant difference in cell viability between the DHNPs and the control ($p > 0.05$). At concentrations of 100, 500, and 1000 μg/mL, DHNPs significantly promoted cell viability ($p < 0.05$), with the effect at 1000 μg/mL being greater than at 100 and 500 μg/mL ($p < 0.05$). However, at 2000 μg/mL, the promotive effect on cell viability decreased. Consequently, DHNPs at a concentration of 1000 μg/mL (corresponding to a caffeic acid concentration of 5.24 μg/mL) and a standard solution of caffeic acid at 5.24 μg/mL (serving as a control) were selected for cellular uptake experiments. Caffeic acid was also used as a representative free polyphenol for comparison with the bound polyphenols within DHNPs in subsequent analyses.

> ⓘ Images may appear blurred during proofing as they have been optimized for fast web viewing. A high quality version will be used in the final publication. Click on the image to view the original version.

alt-text: Fig. 6

Fig. 6. Fig. 6
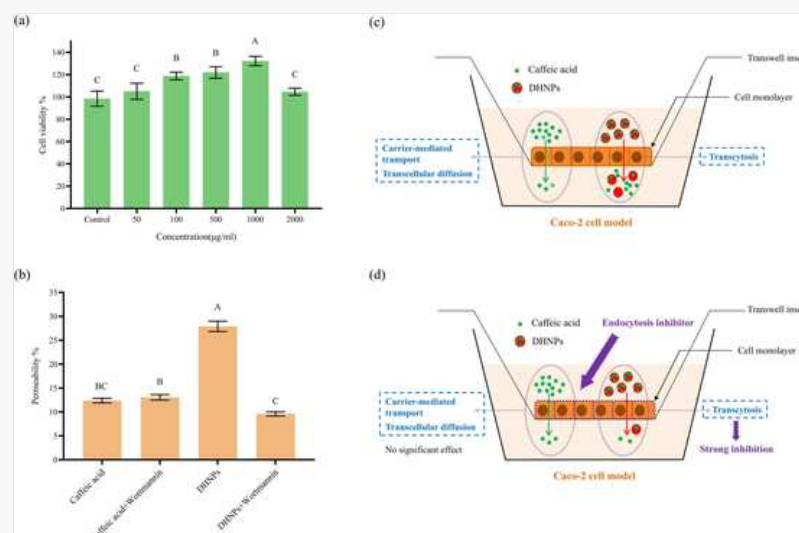
(a) Effects of DHNPs on Caco-2 cell viability; (b) Permeability rates of samples in the Caco-2 monolayer permeability model; (c) Uptake model of caffeic acid by Caco-2 monolayer cells; (d) Changes in caffeic acid uptake by cells after treatment with endocytosis inhibitors. Note: Different letters indicate significant differences at $p < 0.05$.

3.11. 3.11 Effects of DHNPs on polyphenol absorption in Caco-2 cells

The Caco-2 cell monolayer model was used to evaluate the intestinal absorption of caffeic acid, assessing the intestinal absorption of polyphenolic compounds in DHNPs. First, regarding the integrity of the Caco-2 cell monolayer, as shown in Fig. S2, the TEER value of the Caco-2 cell monolayer increased with the extension of the culture time. On day 21, the TEER value reached 421.46 Ω·cm^2, indicating that the integrity of the Caco-2 cell monolayer met the experimental requirements. The permeability results for polyphenols were shown in Fig. 6b, the cell permeability of caffeic acid from DHNPs was 27.90 %, significantly higher than that of the caffeic acid standard at 12.38 % ($p < 0.05$), indicating that the structure of DHNPs facilitated the transport of caffeic acid across the Caco-2 cell monolayer and enhanced its absorption. It has been documented that the cellular uptake of baicalin is significantly improved by the formation of supramolecular assemblies and particulate aggregates. This improvement is hypothesized to stem from the synergistic interactions among a diverse array of components, encompassing flavonoids, alkaloids, glycosides, polysaccharides, and glycoproteins [42]. This phenomenon happened in the processing of dried hawthorn, where the interaction among different components leads to the formation of DHNPs, thereby increasing cellular uptake of caffeic acid.

Additionally, since intestinal epithelial cells typically absorbed large extracellular molecules through endocytosis [65], it was speculated that DHNPs promote caffeic acid uptake *via* endocytosis of Caco-2 cells. To test this hypothesis, cells were treated with DHNPs in the presence of the endocytosis inhibitor wortmannin (a phosphoinositide 3-kinase (PI3K) inhibitor that can block macropinocytosis and phagocytosis in epithelial cells), and the uptake of free caffeic acid was compared with and without the inhibitor. As shown in Fig. 6b, wortmannin had no significant effect on the uptake of free caffeic acid ($p > 0.05$), indicating that its target site was not related to diffusion pathways. However, the uptake of bound caffeic acid within DHNPs significantly decreased ($p < 0.05$) from 27.90 % to 9.58 % upon inhibitor treatment (Figs. 76c-d). Similarly, Nystatin (25 μg/mL), another inhibitor of caveolin-mediated endocytosis (CvME), also used for the permeability assay, leading to a significant reduction in the permeability of DHNP-bound polyphenols, decreasing from 27.90 % to 8.61 % and no significant change on the permeability of free polyphenol (Fig. S1). It also aligned with a previous study [66], which showed that the uptake of curcumin-loaded protein–pectin nanoparticles by Caco-2 cells could be inhibited by multiple endocytosis inhibitors including sucrose, Nystatin, and Wortmannin, with the latter two showing comparable effects. Another study reported the colloidal nanoparticles in lamb soup were primarily absorbed *via* caveolin-dependent endocytosis, macropinocytosis, and phagocytosis [67]. While the specific endocytic routes of DHNPs remained to be fully clarified, these results suggest that the internalization of DHNPs was likely mediated by multiple endocytic pathways, including not only macropinocytosis, but also potentially caveolin-mediated endocytosis. Moreover, endocytosis appeared to play a critical role in the epithelial transport of DHNP-bound polyphenols, thereby potentially enhancing the oral bioavailability of polyphenols.

This study confirmed that structural differences between DHNPs-bound polyphenols and free polyphenols result in distinct cellular uptake behaviors, establishing a preliminary structure–function relationship. However, several limitations remain to be addressed. Firstly, although we employed two representative endocytic inhibitors—Wortmannin (a PI3K inhibitor that significantly reduced the trans-epithelial transport of DHNPs-bound polyphenols) and Nystatin (a caveolin-mediated endocytosis inhibitor)—this study suggested that the uptake of DHNPs likely involved multiple endocytic pathways, rather than relying solely on passive diffusion or classical transporter-mediated mechanisms. Therefore, a more comprehensive elucidation of the endocytic mechanisms was warranted. Secondly, given the complexity of endocytic processes, we have not yet directly identified the specific receptors involved in DHNPs uptake. However, previous studies [68] have reported that membrane receptors such as SR-BI (Scavenger Receptor Class B Type I) can recognize and mediate the uptake of pectin and pectin-like polysaccharides, which may offer a mechanistic clue for receptor-mediated interactions in our system. In addition, recent studies on plant-derived extracellular vesicle-like nanoparticles have shown that terminal galactose residues on their surfaces can facilitate receptor-mediated endocytosis *via* asialoglycoprotein receptors (ASGPRs), particularly in cells such as macrophages. This pathway has been demonstrated in nanoparticles derived from green tea [69], mulberry leaves [70], and other plant sources [71]. Given the compositional and surface similarities, such interactions may also be relevant to DHNPs uptake and warrant further investigation in future studies.

This study revealed the advantages of DHNPs in improving polyphenol stability and absolution, laying the foundation for their application in functional foods and drug delivery. With these properties, DHNPs can be incorporated into functional beverages and dietary supplements to reduce polyphenol degradation and extend health benefits. Additionally, DHNPs aligned with the clean-label food trend. By integrating the "Medicine and Food Homology" concept, this technology enhanced the nutritional value of hawthorn-based processed products, such as instant powders, health drinks, and functional snacks, meeting the demand for nutrition fortification and convenient consumption.

4 Conclusion

This study reveals how herbal processing, particularly drying, chemically modifies hawthorn polyphenols and promotes the formation of natural polyphenol-based nanoparticles (DHNPs), thereby enhancing their stability and absorption. DHNPs exhibited a high polyphenol loading (~25 %) and were stabilized by hawthorn polysaccharides—mainly HG-type pectin—through both non-covalent and covalent interactions. These structural features contribute to controlled release and improved bioavailability compared to free polyphenols. These features facilitate the transformation of hawthorn into high-value functional food products through deep processing, aligning with trends in nutritional enhancement and bioactive delivery. This work provides a new perspective for developing herb-based functional foods by leveraging natural polysaccharides to improve polyphenol delivery.

Supplementary data to this article can be found online at https://doi.org/10.1016/j.ijbiomac.2025.143274.

CRediT authorship contribution statement

Xiangyu Meng: Writing – review & editing, Writing – original draft, Investigation, Data curation. **Sihao Luo:** Writing – review & editing, Visualization, Data curation. **Zhaoshuo Yu:** Writing – review & editing, Supervision, Methodology, Conceptualization. **Fangzhou He:** Visualization. **Hanlin Xu:** Investigation. **Xuanlu Jin:** Investigation. **Lijing Ke:** Supervision, Methodology. **Jianwu Zhou:** Methodology. **Huaiyu Gu:** Conceptualization. **Pingfan Rao:** Validation, Supervision. **Patrick Wall:** Conceptualization.

Declaration of competing interest

The authors declare that they have no known competing financial interests or personal relationships that could have appeared to influence the work reported in this paper.

Q4

Q5 ~~Data availability1~~

~~The authors declare that the data supporting the results of this study are available within the article.~~

References

> ⓘ The corrections made in this section will be reviewed and approved by a journal production editor. The newly added/removed references and its citations will be reordered and rearranged by the production team.

[1] Z. Yu, L. Ke, T. Lu, L. Li, H. Gu, P. Rao, Implementing a food first strategy can transform preventive healthcare, Npj Sci. Food 8 (2024) 57.

[2] L. Wang, X. Zhu, H. Liu, B. Sun, ~~Medicine and food homology substances: A review of bioactive ingredients, pharmacological effects and applications~~Medicine and food homology substances: a review of bioactive ingredients, pharmacological effects and applications, Food Chem. 463 (2025) 141111.

[3] M. Cui, L. Cheng, Z. Zhou, Z. Zhu, Y. Liu, C. Li, B. Liao, M. Fan, B. Duan, ~~Traditional uses, phytochemistry, pharmacology, and safety concerns of hawthorn (Crataegus genus): A comprehensive review~~Traditional uses, phytochemistry, pharmacology, and safety concerns of hawthorn (Crataegus genus): a comprehensive review, J. Ethnopharmacol. 319 (2024) 117229.

[4] M. Li, X. Chen, J. Deng, D. Ouyang, D. Wang, Y. Liang, Y. Chen, Y. Sun, Effect of thermal processing on free and bound phenolic compounds and antioxidant activities of hawthorn, Food Chem. 332 (2020) 127429.

[5] T. Li, S. Fu, X. Huang, X. Zhang, Y. Cui, Z. Zhang, Y. Ma, X. Zhang, Q. Yu, S. Yang, S. Li, ~~Biological properties and potential application of hawthorn and its major functional components: A review~~Biological properties and potential application of hawthorn and its major functional components: a review, J. Funct. Foods 90 (2022) 104988.

[6] Y. Wang, M. Lv, T. Wang, J. Sun, Y. Wang, M. Xia, Y. Jiang, X. Zhou, J. Wan, Research on mechanism of charred hawthorn on digestive through modulating "brain-gut" axis and gut flora, J. Ethnopharmacol. 245 (2019) 112166.

[7] X. Guo, W. Luo, L. Wu, L. Zhang, Y. Chen, T. Li, H. Li, W. Zhang, Y. Liu, J. Zheng, Y. Wang, ~~Natural Products from Herbal Medicine Self-Assemble into Advanced Bioactive Materials~~Natural products from herbal medicine self-assemble into advanced bioactive materials, Adv. Sci. 2403388 (2024).

[8] M.T. El-Saadony, T. Yang, A.M. Saad, S.S. Alkafaas, S.S. Elkafas, G.S. Eldeeb, D.M. Mohammed, H.M. Salem, S.A. Korma, S.A. Loutfy, M.Y. Alshahran, A.E. Ahmed, W.F.A. Mosa, T.A. Abd El-Mageed, A.F. Ahmed, M.A. Fahmy, M.K. El-Tarabily, R.M. Mahmoud, S.F. AbuQamar, K.A. El-Tarabily, J.M. Lorenzo, ~~Polyphenols: Chemistry, bioavailability, bioactivity, nutritional aspects and human health benefits: A review~~Polyphenols: chemistry, bioavailability, bioactivity, nutritional aspects and human health benefits: a review, Int. J. Biol. Macromol. 277 (2024) 134223.

[9] D. Cianciosi, T.Y. Forbes-Hernández, L. Regolo, J.M. Alvarez-Suarez, M.D. Navarro-Hortal, J. Xiao, J.L. Quiles, M. Battino, F. Giampieri, ~~The reciprocal interaction between polyphenols and other dietary compounds: Impact on bioavailability, antioxidant capacity and other physico-chemical and nutritional parameters~~The reciprocal interaction between polyphenols and other dietary compounds: impact on bioavailability, antioxidant capacity and other physico-chemical and nutritional parameters, Food Chem. 375 (2022) 131904.

[10] C. Manach, A. Scalbert, C. Morand, C. Rémésy, L. Jiménez, ~~Polyphenols: Food sources and bioavailability~~Polyphenols: food sources and bioavailability, Am. J. Clin. Nutr. 79 (2004) 727–747.

[11] Y. Shen, N. Zhang, J. Tian, G. Xin, L. Liu, X. Sun, B. Li, Advanced approaches for improving bioavailability and controlled release of anthocyanins, J. Control. Release 341 (2022) 285–299.

[12] L. Mahmutović, A. Sezer, E. Bilajac, A. Hromić-Jahjefendić, V.N. Uversky, U. Glamočlija, ~~Polyphenol stability and bioavailability in cell culture medium: Challenges, limitations and future directions~~Polyphenol stability and bioavailability in cell culture medium: challenges, limitations and future directions, Int. J. Biol. Macromol. 279 (2024) 135232.

[13] F. Weber, Noncovalent Polyphenol–Macromolecule Interactions and Their Effects on the Sensory Properties of Foods, J. Agric. Food Chem. 70 (2022) 72–78.

[14] A.S.P. Moreira, F.M. Nunes, C. Simões, E. Maciel, P. Domingues, M.R.M. Domingues, M.A. Coimbra, ~~Transglycosylation reactions, a main mechanism of phenolics incorporation in coffee melanoidins: Inhibition by Maillard reaction~~Transglycosylation reactions, a main mechanism of phenolics incorporation in coffee melanoidins: inhibition by Maillard reaction, Food Chem. 227 (2017) 422–431.

[15] A.S.P. Moreira, M.A. Coimbra, F.M. Nunes, C.P. Passos, S.A.O. Santos, A.J.D. Silvestre, A.M.N. Silva, M. Rangel, M.R.M. Domingues, ~~Chlorogenic acid–arabinose hybrid domains in coffee melanoidins: Evidences from a model system~~Chlorogenic acid–arabinose hybrid domains in coffee melanoidins: evidences from a model system, Food Chem. 185 (2015) 135–144.

[16] F. He, Z. Yu, S. Luo, X. Meng, L. Wang, X. Jin, Z. Huang, Y. Zhang, P. Deng, W.K. Peng, L. Ke, H. Wang, J. Zhou, P. Wall, P. Rao, Why are clams steamed with wine in Mediterranean cuisine?, Npj Sci. Food 8 (2024) 44.

[17] Y.-H. Miao, X. Wang, X.-M. Zhao, Y.-W. Hu, X. Liu, D.-W. Deng, Co-assembly strategies of natural plant compounds for improving their bioavailability, Food Med. Homol. 2 (2025) 9420022.

[18] J. Zhou, G. Gao, Q. Chu, H. Wang, P. Rao, L. Ke, Chromatographic isolation of nanoparticles from Ma-Xing-Shi-Gan-Tang decoction and their characterization, J. Ethnopharmacol. 151 (2014) 1116–1123.

[19] Z. Yu, Y. Tan, S. Luo, J. Zhou, T. Xu, J. Zou, L. Ke, J. Yu, S. Zhang, J. Zhou, P. Rao, J. Li, Food nanoparticles from rice vinegar: isolation, characterization, and antioxidant activities, Npj Sci. Food 6 (2022) 1–8.

[20] Z. Li, J. Zhang, H. Zhang, Y. Liu, C. Zhu, Effect of different processing methods of hawthorn on the properties and emulsification performance of hawthorn pectin, Carbohydr. Polym. 298 (2022) 120121.

[21] A. Peng, L. Lin, M. Zhao, Discovery, characterization and stability evaluation of self-assembled submicroparticles in chrysanthemum tea infusions, Food Biosci. 47 (2022) 101642.

[22] S. Zhu, J. Ke, X. Li, X. Xu, Y. Liu, R. Guo, J. Chen, Selective hydrolysis of traditional Chinese medicine residue into reducing sugars catalysed by sulfonated carbon catalyst and application of hydrolysate, Chem. Eng. J. 497 (2024) 154586.

[23] C.-H. Zhang, Y.-H. Yun, Z.-M. Zhang, Y.-Z. Liang, Simultaneous determination of neutral and uronic sugars based on UV–vis spectrometry combined with PLS, Int. J. Biol. Macromol. 87 (2016) 290–294.

[24] D.L. Jones, A.G. Owen, J.F. Farrar, Simple method to enable the high resolution determination of total free amino acids in soil solutions and soil extracts, Soil Biol. Biochem. 34 (2002) 1893–1902.

[25] K. Wang, N. Tang, X. Bian, D. Geng, H. Chen, Y. Cheng, Structural characteristics, chemical compositions and antioxidant activity of melanoidins during the traditional brewing of Monascus vinegar, Lwt 209 (2024) 116760.

[26] D.O. Carvalho, E. Correia, L. Lopes, L.F. Guido, Further insights into the role of melanoidins on the antioxidant potential of barley malt, Food Chem. 160 (2014) 127–133.

[27] K. Bu, S. Wu, C. Zhu, M. Wei, Comparative study of HG-type low-ester hawthorn pectin as a promising material for the preparation of hydrogel, Carbohydr. Polym. 296 (2022) 119941.

[28] W. Wang, Y. Wang, F. Chen, F. Zheng, Comparison of determination of sugar-PMP derivatives by two different stationary phases and two HPLC detectors: C18 vs. amide columns and DAD vs. ELSD, J. Food Compos. Anal. 96 (2021) 103715.

[29] P. Rodsamran, R. Sothornvit, Microwave heating extraction of pectin from lime peel: characterization and properties compared with the conventional heating method, Food Chem. 278 (2019) 364–372.

[30] J. Zhang, W. Xin, Y. Zou, J. Yan, W. Tang, Y. Ji, W. Li, Dynamic changes and correlation analysis of microorganisms and flavonoids/ amino acids during white tea storage, Food Chem. 455 (2024) 139932.

[31] C. Coelho, M. Ribeiro, A.C.S. Cruz, M.R.M. Domingues, M.A. Coimbra, M. Bunzel, F.M. Nunes, Nature of phenolic compounds in coffee melanoidins, J. Agric. Food Chem. 62 (2014) 7843–7853.

[32] X. Zhong, S. Zhang, H. Wang, J. Yang, L. Li, J. Zhu, Y. Liu, Ultrasound-alkaline combined extraction improves the release of bound polyphenols from pitahaya (Hylocereus undatus 'foo-Lon') peel: composition, antioxidant activities and enzyme inhibitory activity, Ultrason. Sonochem. 90 (2022) 106213.

[33] Y. Zhang, H. Xiao, X. Lv, C. Zheng, Z. Wu, N. Wang, J. Wang, H. Chen, F. Wei, Profiling and spatial distribution of phenolic compounds in rapeseed by two-step extraction strategy and targeted metabolomics combined with chemometrics, Food Chem. 401 (2023) 134151.

[34] H. Wang, B. Song, J. Zhou, G. Gao, Y. Ding, X. Meng, L. Ke, W. Ding, S. Zhang, T. Chen, P. Rao, Fabrication and characterization of curcumin-loaded nanoparticles using licorice protein isolate from Radix Glycyrrhizae, Int. J. Biol. Macromol. 255 (2024) 128235.

[35] I.F.F. Benzie, J.J. Strain, The ferric reducing ability of plasma (FRAP) as a measure of "antioxidant power": the FRAP assay, Anal. Biochem. 239 (1996) 70–76.

[36] R. Re, N. Pellegrini, A. Proteggente, A. Pannala, M. Yang, C. Rice-Evans, Antioxidant activity applying an improved ABTS radical cation decolorization assay, Free Radic. Biol. Med. 26 (1999) 1231–1237.

[37] R. Dong, S. Liu, J. Xie, Y. Chen, Y. Zheng, X. Zhang, E. Zhao, Z. Wang, H. Xu, Q. Yu, The recovery, catabolism and potential bioactivity of polyphenols from carrot subjected to in vitro simulated digestion and colonic fermentation, Food Res. Int. 143 (2021) 110263.

[38] B. Ou, M. Hampsch-Woodill, R.L. Prior, Development and validation of an improved oxygen radical absorbance capacity assay using fluorescein as the fluorescent probe, J. Agric. Food Chem. 49 (2001) 4619–4626.

[39] M. Molaveisi, M. Shahidi-Noghabi, S. Naji-Tabasi, Vitamin D3-loaded nanophytosomes for enrichment purposes: formulation, structure optimization, and controlled release, J. Food Process Eng. 43 (2020).

[40] X. Jin, T.L. Luong, N. Reese, H. Gaona, V. Collazo-Velez, C. Vuong, B. Potter, J.C. Sousa, R. Olmeda, Q. Li, L. Xie, J. Zhang, P. Zhang, G. Reichard, V. Melendez, S.R. Marcsisin, B.S. Pybus, Comparison of MDCK-MDR1 and Caco-2 cell based permeability assays for anti-malarial drug screening and drug investigations, J. Pharmacol. Toxicol. Methods 70 (2014) 188–194.

[41] C. Chen, T. Li, Z. Chen, L. Wang, X. Luo, Absorption rates and

mechanisms of Avenanthramides in a Caco-2 cell model and their antioxidant activity during absorption, J. Agric. Food Chem. 68 (2020) 2347–2356.

[42] D. Lin, Q. Du, H. Wang, G. Gao, J. Zhou, L. Ke, T. Chen, C. Shaw, P. Rao, Antidiabetic Micro-/nanoaggregates from Ge-gen-Qin-Lian-Tang decoction increase absorption of Baicalin and cellular antioxidant activity in vitro, Biomed. Res. Int. 2017 (2017) 1–8.

[43] A. Ressaissi, M.L.M. Serralheiro, Hydroxycinnamic acid derivatives effect on hypercholesterolemia, comparison with ezetimibe: permeability assays and FTIR spectroscopy on Caco-2 cell line, Curr. Res. Pharmacol. Drug Discov. 3 (2022) 100105.

[44] A. Thiengsusuk, W. Sumsakul, K. NaBangchang, Effects of Atractylodin and β-Eudesmol on P-glycoprotein and Caco-2 cells permeability, Phytomedicine Plus 5 (2025) 100608.

[45] A. Peng, L. Lin, M. Zhao, Chemical basis and self-assembly mechanism of submicroparticles forming in chrysanthemum tea infusion, Food Chem. 427 (2023) 136745.

[46] P. Makvandi, M. Chen, R. Sartorius, A. Zarrabi, M. Ashrafizadeh, F. Dabbagh Moghaddam, J. Ma, V. Mattoli, F.R. Tay, Endocytosis of abiotic nanomaterials and nanobiovectors: inhibition of membrane trafficking, Nano Today 40 (2021) 101279.

[47] X. Ding, Y. Zhang, J. Li, S. Yan, Structure, spectral properties and antioxidant activity of melanoidins extracted from high temperature sterilized lotus rhizome juice, Int. J. Biol. Macromol. 270 (2024) 132171.

[48] L. Roman, M. Guo, A. Terekhov, M. Grossutti, N.P. Vidal, B.L. Reuhs, M.M. Martinez, Extraction and isolation of pectin rich in homogalacturonan domains from two cultivars of hawthorn berry (Crataegus pinnatifida), Food Hydrocoll. 113 (2021) 106476.

[49] D. Sun, X. Chen, C. Zhu, Physicochemical properties and antioxidant activity of pectin from hawthorn wine pomace: a comparison of different extraction methods, Int. J. Biol. Macromol. 158 (2020) 1239–1247.

[50] S. Zhang, Z. He, Y. Cheng, F. Xu, X. Cheng, P. Wu, Physicochemical characterization and emulsifying properties evaluation of RG-I enriched pectic polysaccharides from Cerasus humilis, Carbohydr. Polym. 260 (2021) 117824.

[51] X. Wang, Y. Sun, Y. Yu, D. Huang, Y. Liu, M. Huang, Y. Jiang, D. Li, Sequential extraction of hawthorn pectin: an attempt to reveal their original mode of being in plants and functional properties, Int. J. Biol. Macromol. 282 (2024) 136756.

[52] F.M. Nunes, M.A. Coimbra, Melanoidins from coffee infusions. Fractionation, chemical characterization, and effect of the degree of roast, J. Agric. Food Chem. 55 (2007) 3967–3977.

[53] A.S.P. Moreira, F.M. Nunes, M.R. Domingues, M.A. Coimbra, Coffee melanoidins: structures, mechanisms of formation and potential health impacts, Food Funct. 3 (2012) 903–915.

[54] L. Lin, S. Peng, X. Chen, C. Li, H. Cui, Silica nanoparticles loaded with caffeic acid to optimize the performance of cassava starch/sodium carboxymethyl cellulose film for meat packaging, Int. J. Biol. Macromol. 241 (2023) 124591.

[55] Z. Chen, Y. Ma, L. Gou, S. Zhang, Z. Wang, Construction of caffeic acid modified porous starch as the dual-functional microcapsule for encapsulation and antioxidant property, Int. J. Biol. Macromol. 228 (2023) 358–365.

[56]

U. Kannamangalam Vijayan, N.N. Shah, A.B. Muley, R.S. Singhal, ~~Complexation of curcumin using proteins to enhance aqueous solubility and bioaccessibility: Pea protein vis-à-vis whey protein~~Complexation of curcumin using proteins to enhance aqueous solubility and bioaccessibility: pea protein Vis-à-Vis whey protein, J. Food Eng. 292 (2021) 110258.

[57] M. García-Alonso, S. De Pascual-Teresa, C. Santos-Buelga, J.C. Rivas-Gonzalo, Evaluation of the antioxidant properties of fruits, Food Chem. 84 (2004) 13–18.

[58] N. Yang, R. Qiu, S. Yang, K. Zhou, C. Wang, S. Ou, J. Zheng, Influences of stir-frying and baking on flavonoid profile, antioxidant property, and hydroxymethylfurfural formation during preparation of blueberry-filled pastries, Food Chem. 287 (2019) 167–175.

[59] X. Lou, H. Xu, M. Hanna, L. Yuan, Identification and quantification of free, esterified, glycosylated and insoluble-bound phenolic compounds in hawthorn berry fruit (Crataegus pinnatifida) and antioxidant activity evaluation, Lwt 130 (2020) 109643.

[60] M. Stanciauskaite, M. Poskute, V. Kurapkiene, M. Marksa, V. Jakstas, L. Ivanauskas, M. Kersiene, D. Leskauskaite, K. Ramanauskiene, ~~Optimization of Delivery and Bioavailability of Encapsulated Caffeic Acid~~Optimization of delivery and bioavailability of encapsulated Caffeic acid, Foods 12 (2023) 1993.

[61] M.P. Paarakh, P.A.N.I. Jose, C.M. Setty, ~~G. V~~G.V. Peter, ~~Release Kinetics — Concepts and Applications~~Release kinetics – concepts and applications, Int. J. Pharm. Res. Technol. 8 (2019) 12–20.

[62] P. Prasher, M. Sharma, M. Mehta, S. Satija, A.A. Aljabali, M.M. Tambuwala, K. Anand, N. Sharma, H. Dureja, N.K. Jha, G. Gupta, M. Gulati, S.K. Singh, D.K. Chellappan, K.R. Paudel, P.M. Hansbro, K. Dua, Current-status and applications of polysaccharides in drug delivery systems, Colloid Interface Sci. Commun. 42 (2021) 100418.

[63] ~~E. Türkeş, Y. Sağ Açıkel, Folic acid-conjugated cancer drug curcumin-loaded albumin nanoparticles: Investigation of curcumin release kinetics, J. Drug Deliv. Sci. Technol. 91 (2024) 105178.~~E. Türkeş, Y. Sağ Açıkel, Folic acid-conjugated cancer drug curcumin-loaded albumin nanoparticles: investigation of curcumin release kinetics, J. Drug Deliv. Sci. Technol. 91 (2024) 105178.

[64] Z. Yaneva, N. Georgieva, ~~Physicochemical and morphological characterization of pharmaceutical nanocarriers and mathematical modeling of drug encapsulation/release mass transfer processes, in: Nanoscale Fabr~~Physicochemical and Morphological Characterization of Pharmaceutical Nanocarriers and Mathematical Modeling of Drug Encapsulation/Release Mass Transfer Processes, in: Nanoscale Fabr, Elsevier, Optim. Scale-Up Biol. Asp. Pharm. Nanotechnol, 2018, pp. 173–218.

[65] J. Fu, S. Li, M. Xu, L. Liu, L. Chen, D. Zhang, Absorption and transport mechanism of colloidal nanoparticles (CNPs) in lamb soup based on Caco-2 cell, Food Chem. 463 (2025) 141196.

[66] Y. Liu, J. Zhuang, X. Zhang, C. Yue, N. Zhu, L. Yang, Y. Wang, T. Chen, Y. Wang, L.W. Zhang, Autophagy associated cytotoxicity and cellular uptake mechanisms of bismuth nanoparticles in human kidney cells, Toxicol. Lett. 275 (2017) 39–48.

[67] J. Fu, S. Li, M. Xu, L. Liu, L. Chen, D. Zhang, Absorption and transport mechanism of colloidal nanoparticles (CNPs) in lamb soup based on Caco-2 cell, Food Chem. 463 (2025) 141196.

[68] A.S. Lokhande, P. Jahagirdar, P. Dandekar, P. V. Devarajan, Scavenger Receptor and Targeting Strategies, in: Springer, Cham, 2019: pp. 297–321.

[69] M. Zu, D. Xie, B.S.B. Canup, N. Chen, Y. Wang, R. Sun, Z. Zhang, Y. Fu, F. Dai, B. Xiao, 'Green' nanotherapeutics from tea leaves for orally targeted prevention and alleviation of colon diseases, Biomaterials 279 (2021) 121178.

[70] L. Ma, Y. Ma, Q. Gao, S. Liu, Z. Zhu, X. Shi, F. Dai, R.L. Reis, S.C. Kundu, K. Cai, B. Xiao, ~~Mulberry Leaf Lipid Nanoparticles: a Naturally Targeted CRISPR/Cas9 Oral Delivery Platform for Alleviation of Colon Diseases~~Mulberry leaf lipid nanoparticles: a naturally targeted CRISPR/Cas9 Oral delivery platform for alleviation of Colon diseases, Small 20 (2024) 1–17.

[71]

A. Kilasoniya, L. Garaeva, T. Shtam, A. Spitsyna, E. Putevich, B. Moreno-Chamba, J. Salazar-Bermeo, E. Komarova, A. Malek, M. Valero, D. Saura, ~~Potential of Plant Exosome Vesicles from Grapefruit (Citrus × paradisi) and Tomato (Solanum lycopersicum) Juices as Functional Ingredients and Targeted Drug Delivery Vehicles~~ Potential of plant exosome vesicles from grapefruit (Citrus × paradisi) and tomato (Solanum lycopersicum) juices as functional ingredients and targeted drug delivery vehicles, Antioxidants 12 (2023).
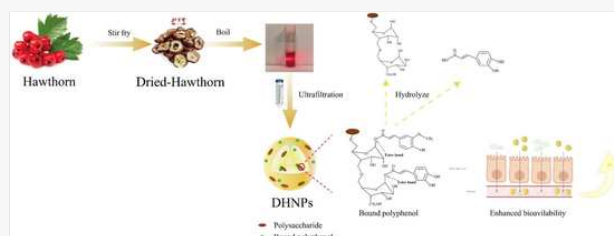
Graphical abstract

Formation of polyphenol-loaded nanoparticles in dried hawthorn and their impact on *in vitro* intestinal absorption.

Images may appear blurred during proofing as they have been optimized for fast web viewing. A high quality version will be used in the final publication. Click on the image to view the original version.

alt-text: Unlabelled Image

To clearly illustrate changes in the composition of polyphenolic compounds before and after saponification, a volcano plot (Fig. 2c) was used, where each point represents a compound, and the relative increase or decrease in content was expressed as Log2 (after saponification/before saponification). Table S1 showed the molecular formulas, classifications, mass-to-charge ratios, and relative content variations of all compounds in DHNPs. Based on the data, most phenolic compounds showed an increase in relative content after saponification, including caffeic acid, hyperoside, (—)-catechin, morin, 2,5-dihydroxybenzoic acid, cinchonain 1a, trans-ferulic acid, and cleomiscosin A. This increase likely explained the overall rise in total polyphenol content (Fig. 2a). The saponification reaction broke the ester bonds and other covalent bonds between the DHNPs matrix and polyphenols (Fig. 2d), leading to an increase in many phenolic compounds, further confirming the presence of covalently bound polyphenols in DHNPs. Additionally, the relative content of certain phenolic compounds, such as chlorogenic acid, decreased after saponification (Table S1). This reduction was attributed to alkaline saponification breaking the ester bonds within the chlorogenic acid molecule, leading to simpler polyphenolic substances like caffeic acid (Fig. 2d). Carina Coelho et al. suggested that saponification could dissociate both the simple adsorbed and covalently condensed chlorogenic acid in coffee melanoidin, simultaneously degrading it and releasing it as caffeic acid [31], which aligned the results here.

The following are the supplementary data related to this article.

📄 Multimedia Component 1

~~Table S1.~~Table S1

Identification of SHNPs Compound Types.

alt-text: Table S1

📄 Multimedia Component 2

Supplementary figures

alt-text: Image 1

Queries and Answers

Q1

Query: Your article is being processed as a regular item to be included in a **regular issue**. Please confirm if this is correct or if your article should be published in a special issue using the responses below.

Answer: No

Q2

Query: Please review the **given names** (no colouring) **and surnames** (highlighted in teal colouring) to make sure that we have identified them correctly and that they are presented in the desired order. Carefully verify the spelling of all authors' names as well. If changes are needed, please provide the edits in the author section.

Answer: Yes

Q3

Query: Please check whether the **hierarchy of the section headings** is as expected. If changes are needed, please use the comment option to indicate the required changes.

Answer: Reviewed

Q4

Query: Have we correctly interpreted the following funding source(s) and country names you cited in your article: "China Scholarship Council".

Answer: Yes

Q5

Query: We have received two sets of Data Availability statement for your article. As these two are contradicting content, please check and delete either one of them from the article.

Answer: Yes, we have delete the one.

Q6

Query: Please add the **volume number and page range** for the bibliography in reference. Ref. [44].

Answer: Done